ISSN 1070-3284, Russian Journal of Coordination Chemistry, 2020, Vol. 46, No. 5, pp. 365–370. © Pleiades Publishing, Ltd., 2020.

Syntheses, Crystal Structure, and Magnetic Property of a New Mn(II) Complex with an Aromatic *N*-Heterocyclic Tetracarboxylic Acid Ligand

X. F. Liu[a], *, N. N. Ma[a], F. Feng[a], M. D. You[a], and X. Feng[a], **

[a] *College of Chemistry and Chemical Engineering, and Henan Key Laboratory of Function-Oriented Porous Materials, Luoyang Normal University, Luoyang, 471934 P.R. China*

**e-mail: liuxinfang6@126.com*

***e-mail: fengx@lynu.edu.cn*

Received May 12, 2019; revised May 31, 2019; accepted September 17, 2019

Abstract—A new 2D Mn(II) complex named as $[Mn_3(HL)_2(H_2O)_6]_n$ (**I**) (H_4L = 3-(2,4-dicarboxyphenyl)-2,6-dicarboxypyridine) was synthesized and characterized by IR, elemental analysis, and single-crystal X-ray diffraction method (CIF file CCDC no. 1915189). The complex crystallizes in the monoclinic space group $C2/c$ with $Z = 4$, $a = 20.6597(11)$, $b = 9.0949(5)$, $c = 20.6041(12)$ Å, $\beta = 110.056(6)°$. The crystal consists of trinuclear Mn(II) ion clusters $\{Mn_3\}$ which are linked by four independent HL^{3-} ligands and these trimeric units are connected into 2D structure by pentadentate HL^{3-} ligand in alternate bis(bridging) and chelated coordination modes. Thermogravimetry, powder X-ray diffraction, and magnetic measurement experiments are also carried out to determinethe thermal stability, phase purity and magnetism. The results show that weak antiferromagnetic interactions occur between the Mn(II) centers within bridging trinuclear $\{Mn_3\}$ cluster.

Keywords: $\{Mn_3\}$ cluster, *N*-heterocyclic tetracarboxylic acid, single crystal X-ray diffraction, magnetism

DOI: 10.1134/S1070328420050036

INTRODUCTION

The rational design and synthesis of coordination polymers have been attracting more and more researchers in recent decades because of their fascinating topological structure and potential applications in many fields, such as magnetism, luminescence, and catalysis [1–9]. A key factor for the preparation of polymeric complexes is the appropriate selection of organic ligand [10–12]. Aromatic *N*-heterocyclic polycarboxylic acids are one of the valuable ligands because they combine the advantages of azo-heterocyclic and carboxyl groups and have been widely used as multifunctional linkers in the synthesis of coordinate polymers with diverse structures and interesting properties [13–15]. In addition, the carboxyl and azo-heterocyclic groups could serve as hydrogen bond donors and/or acceptors and play an important role in the self-assembly of hydrogen-bond-mediated supramolecular network. Besides the ligand array, the coordination mode and potential applications of coordination polymers also heavily depends on the correct choice of metal center [16, 17]. We are interested in Mn(II) complexes because the Mn(II) ion could be coordinated to O and N atoms singularly or concurrently in solution and some Mn(II) complexes are potential magnetic material or catalyst [18–27].

Considering these factors, we report the synthesis and properties of a newt rinuclear Mn(II) complex $[Mn_3(HL)_2(H_2O)_6]_n$ (**I**) based on 3-(2,4-dicarboxyphenyl)-2,6-dicarboxypyridine (H_4L, Scheme 1) ligand. The complex exhibits a 2D structure, and neighboring 2D layers are connected into 3D network structure by intermolecular hydrogen bonds. The powder X-ray diffraction (PXRD), thermal stability and magnetic property of the complex are also studied.

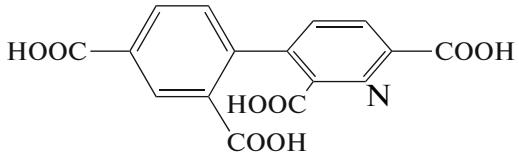

Scheme 1.

EXPERIMENTAL

Materials and methods. All chemicals were obtained from commercial sources and were used without further purification. Infrared spectrum was recorded at room temperature by a FT-IR200 Fourier infrared spectrometer. PXRD patterns were recorded with a Bruker Bruker D8-advance X-ray diffractometer with CuK_α ($\lambda = 1.5418$ Å) radiation. Thermogravimetry (TG) analysis was carried out using an Exstar

Table 1. Crystallographic data and refinement parameters of complex **I**

Parameter	Value
Fw	929.33
Color; crystal form	Yellow; block
Crystal system	Monoclinic
Space group	*C*2/*c*
a, Å	20.6597(11)
b, Å	9.0949(5)
c, Å	20.6041(12)
β, deg	110.056(6)
V, Å^3	3636.7(4)
Z	4
ρ_{calcd}, g cm^{-3}	1.653
μ, mm^{-1}	1.117
F(000)	1785.4
Crystal size, mm	0.18 × 0.19 × 0.20
θ Range for data collection, deg	6.9–56.02
Index range	$-24 \le h \le 26$, $-9 \le k \le 11$, $-26 \le l \le 25$
Reflections collected/unique (R_{int})	7503/3191 (0.0216)
Goodness of fit on F^2	1.095
Reflections with $I > 2\sigma(I)$	2743
R_1, wR_2 ($I > 2\sigma(I)$)	0.0406, 0.1006
R_1, wR_2 (all data)	0.0473, 0.1038
Largest diff. peak/hole, e Å^{-3}	5.61/–0.64

6000 analyzer in Nitrogen at a heating rate of 15°C min^{-1} during the temperature range of 30 to 800°C. Magnetization rate is measured on mpms-7 SQUID magnetic measurement system.

Synthesis of complex I. $Mn(OAc)_2 \cdot 4H_2O$ (0.2 mmol, 0.037 g), H_4L (0.1 mmol, 0.033 g), and water (6.0 mL) was sealed in a 25 mL Teflon-lined stainless steelvessel and heated at 150°C for 72 h. And then the mixture was cooled to room temperature within 72 h. Pale-pink block crystal of complex **I** was isolated after filtration, washed by distilled water and dried naturally in the air. The yield was 65%.

IR (ν, cm^{-1}): 3108 w, 1661 m, 1596 s, 1557 m, 1416 m, 1388 s, 1314 w, 1249 s, 1194 w, 1124 w, 1010 m, 880 w, 855 m, 800 m, 770 s, 690 s.

For $C_{30}H_{24}N_2O_{22}Mn_3$			
Anal. calcd., %	C, 38.77	H, 2.60	N, 3.01
Found, %	C, 37.68	H, 2.52	N, 2.86

X-ray crystallography. The crystal structure of complex **I** was measured using a Bruker SMART APEX CC ray single crystal diffractometer (MoK_α, λ = 0.71073 Å) at room temperature. Using Olex2 [28], the structure was solved with the SIR2004 [29] structure solution program using direct methods and refined with the ShelXL [30] refinement package using Least Squares minimisation. The crystallographic structure data and refinement parameters are listed in Table 1, and the selected bond distances and bond angles are listed in Table 2.

The supplementary crystallographic data for structure **I** has been deposited with the Cambridge Crystallographic Data Centre (no. 1915189; deposit@ccdc.cam.ac.uk or http://www.ccdc.cam.ac. uk/data_request/cif).

RESULTS AND DISCUSSION

X-ray diffraction analysis of complex **I** is carried out and the crystal structure is shown in Fig. 1. The figure shows that there are two crystallographically independent Mn(II) ions (Mn(1) and Mn(2)) in the asymmetric unit of complex **I**. The Mn(1) ion is coordinated by four O(COO$^-$) atoms (O(3a), O(3a)*C* and O(7)*A*, O(7)*B*) from the dicarboxyphenyl and dicarboxypyridine groups of four different HL^{3-} ligands, respectively, as well as two O(*w*) atoms (O(11) and O(11*C*)) to form a disordered octahedral geometry.

Table 2. Selected bond distances (Å) and bond angles (deg) for complex **I**

Bond	*d*, Å	Bond	*d*, Å
Mn(1)–O(7)*A*	2.239(4)	Mn(2)–O(4)	2.072(5)
Mn(1)–O(7)*B*	2.239(4)	Mn(2)–N(1*A*)	2.196(5)
Mn(1)–O(3a)	2.122(6)	Mn(2)–O(6*A*)	2.200(6)
Mn(1)–O(3a)*C*	2.122(6)	Mn(2)–O(7*A*)	2.295(5)
Mn(1)–O(11)	2.164(6)	Mn(2)–O(9)	2.174(5)
Mn(1)–O(11*C*)	2.164(6)	Mn(2)–O(10)	2.188(5)
Angle	ω, deg	Angle	ω, deg
O(7)*B*Mn(1)O(7)*A*	164.23(13)	N(1*)A*Mn(2)O(10)	89.79(10)
O(11)Mn(1)O(7)*A*	83.20(9)	O(10)Mn(2)O(7)*A*	85.35(9)
O(11)Mn(1)O(7)*B*	85.22(9)	O(10)Mn(2)O(6)*A*	94.04(10)
O(11)*C* Mn(1)O(11)	85.4(2)	O(4)Mn(2)O(7)*A*	107.18(9)
O(3a)Mn(1)O(7)*A*	95.6(3)	O(4)Mn(2)O(6)*A*	107.82(10)
O(3a)Mn(1)O(7)*B*	97.1(3)	O(4)Mn(2)N(1)*A*	175.24(11)
O(3a)Mn(1)O(11)*C*	173.8(3)	O(4)Mn(2)O(10)	85.46(11)
O(3a)Mn(1)O(11)	100.8(3)	O(4)Mn(2)O(9)	93.89(12)
O(3a)*C*Mn(1)O(3a)	73.0(5)	O(9)Mn(2)O(7)*A*	89.66(11)
O(6)*A* Mn(2)O(7)*A*	144.83(8)	O(9)Mn(2)O(6)*A*	91.34(11)
N(1)*A* Mn(2)O(7)*A*	72.21(8)	O(9)Mn(2)N(1)*A*	90.83(11)
N(1)*A* Mn(2)O(6)*A*	72.62(9)	O(9(Mn(2)O(10)	174.52(11)

* Symmetry transformations used to generate equivalent atoms: (*A*) $1.5 - x$, $-0.5 + y$, $1.5 - z$; (*B*) $-0.5 + x$, $-0.5 + y$, z; (*C*) $1 - x$, y, $1.5 - z$.

The Mn(2) ion also exhibits a disordered octahedral [NO_5] geometry coordinated by two O(COO^-) atoms (O(6)*A* and O(7)*A*) and one N(1)*A*(Py) atom in chelated pentatomic double-ring configuration, one O(COO^-) atom (O(4)) from the other HL^{3-} ligand and two O(*w*) (O(9) and O(10)). It is noticeable that three symmetric Mn(II) ions (Mn(2), Mn(1), and Mn(2)*C*) are connected into a triple-core cluster {Mn_3} with a Mn–Mn distance of 3.7305(2) Å by two O(COO^-)atoms (O(7)*A* and O(7)*B*) in double-bridge mode. Unsurprisingly, the bond distances of some Mn–O(COO^-) bonds (Mn(1)–O(3a)*A*, Mn(1)–O(3a)*B* 2.122(6), Mn(2)–O(4) 2.072(5) Å) are slightly shorter than those of Mn–O(*w*) bonds (2.164(6)–2.188(5) Å) demonstrating that the deprotonated carboxylate oxygen atoms have a stronger coordination effect with the Mn(II) centre. However, the bond distances of the other few Mn–O(COO^-) bonds (Mn(1)–O(7)*A*, Mn(1)–O(7)*B* 2.239(4), Mn(2)–O(6)*A* 2.200(6), and Mn(2)–O(7)*A* 2.295(5) Å) are longer than those of Mn–O(*w*) bonds. The weak coordination effect between Mn(II) ion and O(COO^-) atom may be caused by the simultaneous coordination of O(7) with two Mn(II) ions and the "electron delocalization" between O(7) and O(6), which decreases the electron density around O(7) and O(6).

Neighbouring triple-core clusters {Mn_3} are linked into 2D structure by pentadentate HL^{3-} ligands in alternant bis(bridging) and chelated pentatomic double-ring coordination modes (Fig. 1 and Fig. 2), which are further connected into 3D supramolecular network by intermolecular hydrogen bonds O(10)–H(10)*B*···O(6)*D* (O···O 2.728(4) Å, angle OHO 157°, (*D*): x, $-1 + y$, z) and O(9)–H(9)*B*···O(2)*E* (O···O 2.761(3), angle OHO 165°, (*E*): $0.5 + x$, $0.5 - y$, $0.5 + z$) (Fig. 3).

To verify the purity of complex **I**, the PXRD pattern was recorded at room temperature (Fig. 4). The figure demonstrates that the experimental patterns have similar intensity and position with the simulated patterns in key positions, which indicates that complex **I** has good purity and can be used for subsequent TG and magnetic susceptibility experiments.

The thermal stability of complex **I** was determined by TG analysis and shown in Fig. 5. Complex **I** shows a weight loss of 11.25% over the temperature range of 30 to 270°C ascribing to the loss of six coordination water molecules (calcd. 11.63%). When the temperature is raised to 326°C, there is an obvious weight loss corresponding to the complete decomposition of organic ligands. The final residue was considered to be manganese oxide (MnO) who account for 22.32% (calcd. 22.90%).

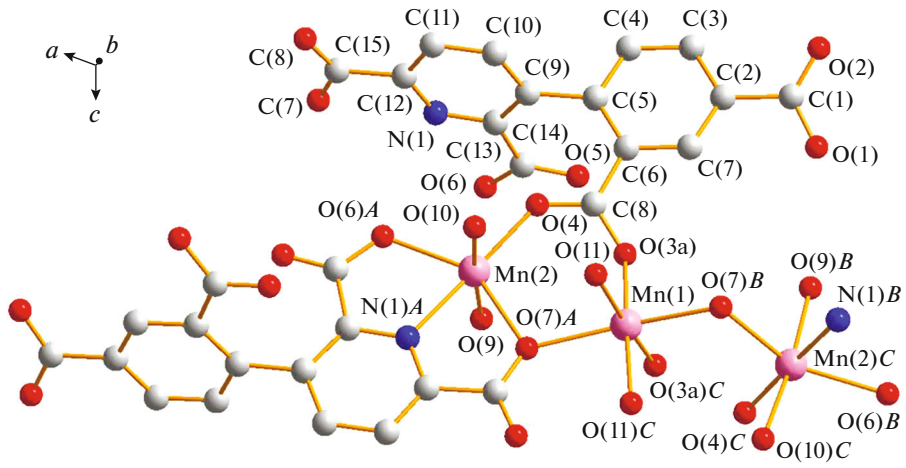

Fig. 1. Structure of trinuclear units in complex **I**: (*A*) 1.5 – *x*, –0.5 + *y*, 1.5 – *z*; (*B*) –0.5 + *x*, –0.5 + *y*, *z*; (*C*) 1 – *x*, *y*, 1,5 – *z*). Hydrogen atoms are omitted for clarity.

Based on the structure analysis of complex **I**, the internuclear Mn(II)···Mn(II) distance in each $\{Mn_3\}$ cluster is 3.7305(2) Å. It could be assumed that the main magnetic interactions occur between the Mn(II) centres. The magnetic susceptibility of complex **I** was measured in the temperature range of 2–300 K under a magnetic field of 2000 Oe. The $\chi_M T$ (and χ_M) versus T and $1/\chi_M$ versus T (inset) curves are shown in Fig. 6. With the decrease of temperature, $\chi_M T$ value decreases smoothly from 300 to 75 K, and then decreases sharply to a minimum value of 5.28 cm^3 K mol^{-1} at 2 K. The drop of $\chi_M T$ value with decreasing temperature may be attributed to the weak antiferromagnetic interactions and the zero-field splitting term of the Mn(II) ion. The $1/\chi_M$ versus T curve (inset) conform to the Curie–Weiss law ($1/\chi_M = (T - \theta)/C$) with the Curie constant of $C = 16.42$ cm^3 K mol^{-1} and the Weiss constant of $\theta = -12.02$ cm^3 K mol^{-1} [31–33]. The negative Weiss constant also indicates the antiferromagnetic interactions between the Mn(II) centres within the trinuclear $\{Mn_3\}$ cluster linked by bridging HL^{3-} ligand.

Thus, a 2D Mn(II) complex containing 3-(2,4-dicarboxyphenyl)-2,6-dicarboxypyridine) (H_4L) ligand, namely, $[Mn_3(HL)_2(H_2O)_6]_n$ (**I**) was synthesized and characterized by IR, elemental analysis and single-crystal X-ray diffraction methods. Three independent Mn(II) ions are linked into trinuclear $\{Mn_3\}$ clusters by four HL^{3-} ligands which are linked into 2D structure by HL^{3-} ligands in alternant bis(bridging) and chelate coordination modes. Neighboring 2D layers are further connected into 3D supramolecular network by intermolecular hydrogen bonds. The PXRD patterns, thermal stability and magnetic property of the complex are also described. The variable temperature magnetic study of complex **I** indicates that there are weak antiferromagnetic interactions between the

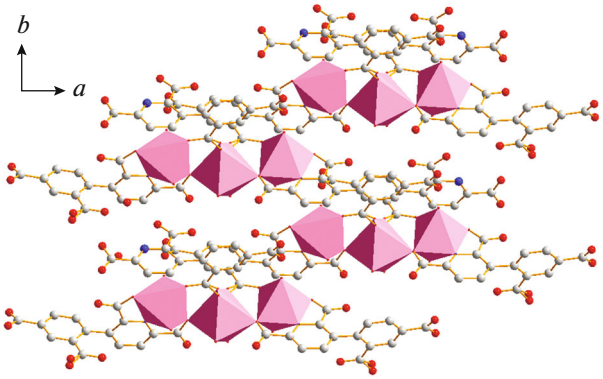

Fig. 2. 2D structure of complex **I** containing trinuclear Mn(II) clusters $\{Mn_3\}$ viewed form c direction.

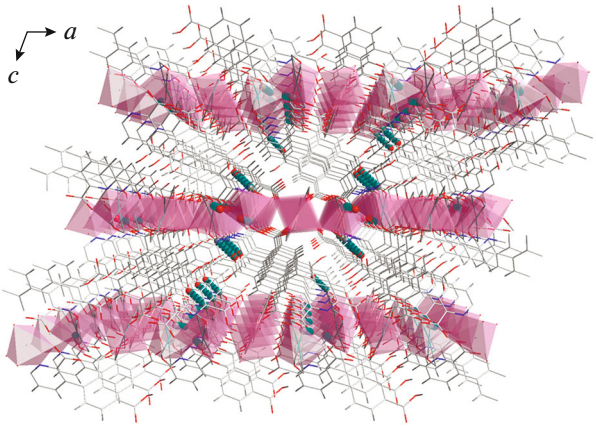

Fig. 3. 3D supramolecular network of complex **I** linked by intermolecular hydrogen bonds viewed form *b* direction.

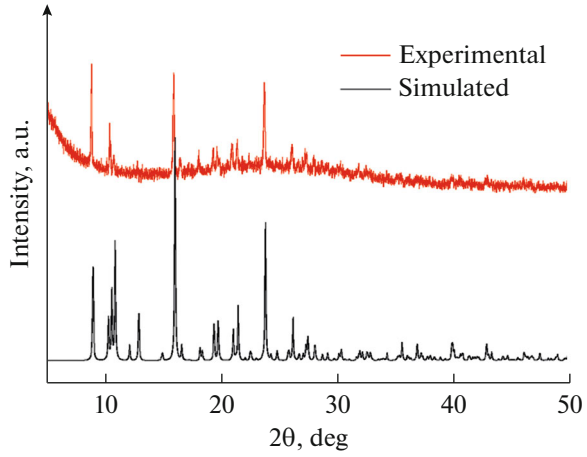

Fig. 4. PXRD patterns of complex **I**.

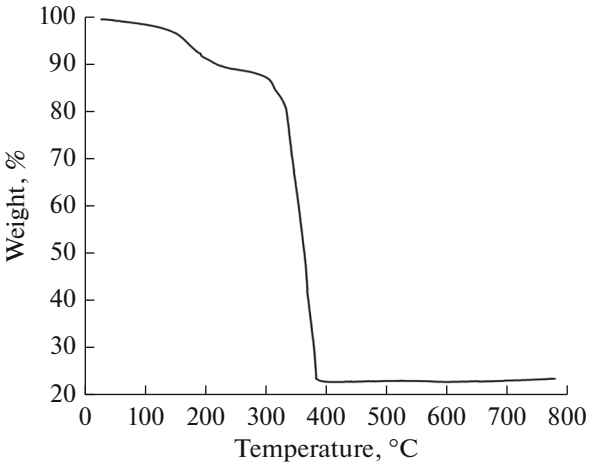

Fig. 5. TG curve of complex **I**.

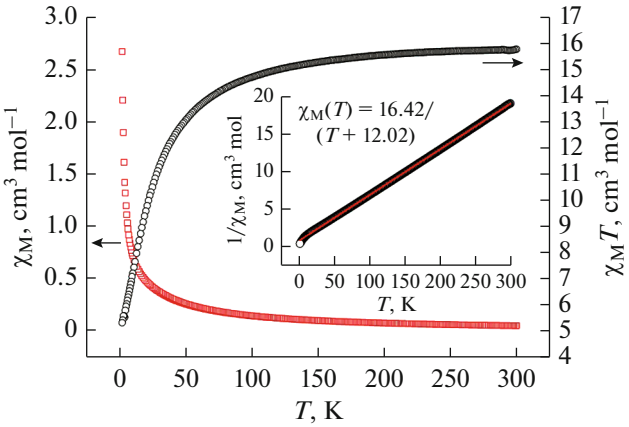

Fig. 6. Temperature dependence of χ_M (○), $\chi_M T$ (□), and $1/\chi_M$ (inset) for complex **I**.

Mn(II) centers within the bridging trinuclear $\{Mn_3\}$ cluster.

FUNDING

The authors are grateful for the financial support from the National Natural Science Foundation of China (nos. U1604143 and U1804131), Training Program for Young Cadre Teachers of Higher Education Institutions in Henan Province (no. 2018GGJS128), and Science and Technology Development Project in Henan Province (no. 172101410037).

REFERENCES

1. Zhao, Y., Yang, X.G., Lu, X.M., et al., *Inorg. Chem.*, 2019, vol. 58, p. 6215.
2. Wang, Y.F., Sun, Y.C., Zhao, J.S., et al., *CrystEngComm*, 2013, vol. 15, no. 46, p. 9980.
3. Mu, Y.Q., Zhu, B.F., Li, D.S., et al., *Inorg. Chem. Commun.*, 2013, vol. 33, p. 86.
4. Fu, H.R., Wang, N., Qin, J.H., et al., *Chem. Commun.*, 2018, vol. 54, p. 11645.
5. Wen, G., Han, M.L., Wu, X.Q., et al., *Dalton Trans.*, 2016, vol. 45, p. 15492.
6. Liu, X.F., Li, R.F., Feng, X., et al., *New. J. Chem.*, 2016, vol. 40, no. 1, p. 619.
7. Bai, L., Wang, H.B., Li, D.S., et al., *Inorg. Chem. Commun.*, 2014, vol. 44, p. 188.
8. Han, M.L., Duan, Y.P., Li, D.S., et al., *Dalton Trans.*, 2014, vol. 43, p. 17519.
9. Zhou, Z., Han, M.L., Fu, H.R., et al., *Dalton Trans.*, 2018, vol. 47, no. 15, p. 5359.
10. Yang, X.G., Ma, L.F., and Yan, D.P., *J. Mater. Chem., A*, 2016, vol. 4, no. 11, p. 3991.
11. Ma, L.F., Qin, J.H., Wang, L.Y., et al., *RSC Adv.*, 2011, vol. 1, no. 2, p. 180.
12. Wang, Y.F., Chen, J.Q., and Geng, J.L., *Z. Anorg. Allg. Chem.*, 2014, vol. 640, no. 10, p. 2086.
13. Liu, X.F., Li, R.F., and Zhang, X.Y., *Russ. J. Coord. Chem.*, 2013, vol. 39, no. 8, p. 593. https://doi.org/10.1134/S1070328413080058
14. Wang, H., Huang, C., Han, Y., et al., *Dalton Trans.*, 2016, vol. 45, p. 7776.
15. Li, X.L., Liu, G.Z., Xin, L.Y., et al., *CrystEngComm*, 2012, vol. 14, no. 5, p. 1729.
16. Kai, S., Sakuma, Y., Mashiko, T., et al., *Inorg. Chem.*, 2017, vol. 56, no. 20, p. 12652.
17. Dong, W.W., Li, D.S., Zhao, J., et al., *CrystEngComm*, 2013, vol. 15, no. 27, p. 5412.
18. Mahapatra, P., Drew, M.G., and Ghosh, A., *Inorg. Chem.*, 2018, vol. 57, no. 14, p. 8338.
19. Du, L., Yu, S., and Liu, X., *New J. Chem.*, 2018, vol. 42, no. 6, p. 4553.
20. Qin, J.H., Wang, H.R., Pan, Q., et al., *Dalton Trans.*, 2015, vol. 44, p. 17639.
21. Khannam, M., Weyhermuller, T., Goswami, U., et al., *Dalton Trans.*, 2017, vol. 46, no. 31, p. 10426.
22. Li, X.L., Liu, G.Z., Xin, L.Y., et al., *J. Solid State Chem.*, 2017, vol. 246, p. 252.

23. Chang, X.H., Qin, J.H., Han, M.L., et al., *CrystEngComm*, 2014, vol. 16, no. 5, p. 870.
24. Li, G.L., Yin, W.D., Li, X.L., et al., *Syn. React. Inorg. Met. Org. Chem.,* 2015, vol. 45, no. 6, p. 869.
25. Chakraborty, P., Majumder, I., Banu, K.S., et al., *Dalton Trans.*, 2016, vol. 45, no. 2, p. 742.
26. Ma, L.F., Han, M.L., Qin, J.H., et al., *Inorg.Chem.*, 2012, vol. 51, no. 17, p. 9431.
27. Zhao, Y., Chang, X.H., Liu, G.Z., et al., *Cryst. Growth. Des.*, 2015, vol. 15, no. 2, p. 966.
28. Dolomanov, O.V., Bourhis, L.J., Gildea, R.J., et al., *J. Appl. Cryst.*, 2009, vol. 42, p. 339.
29. Sheldrick, G.M., *Acta Crystallogr., Sect. A: Found. Adv.*, 2015, vol. 71, p. 3.
30. Sheldrick, G.M., *Acta Crystallogr., Sect. C:, Struct. Chem.*, 2015, vol. 71, p. 3.
31. Lim, K.S., Song, J.H., Kang, D.W., et al., *Dalton Trans.*, 2018, vol. 47, no. 3, p. 845.
32. Berezin, A.S., Vinogradova, K.A., Nadolinny, V.A., et al., *Dalton Trans.*, 2018, vol. 47, no. 5, p. 1657.
33. Kang, H.X., Fu, Y.Q., Ju, F.Y., et al., *Russ. J. Coord. Chem.*, 2018, vol. 44, p. 340. https://doi.org/10.1134/S1070328418050020